Reduced-Feedback Scheduling Policies for Energy-efficient MAC

Priyadarshi Mukherjee[1] and Swades De[2]
[1]Department of Electrical and Computer Engineering, University of Cyprus
[2]Department of Electrical Engineering, Indian Institute of Technology Delhi, New Delhi, India
Emails: mukherjee.priyadarshi@ucy.ac.cy, swadesd@ee.iitd.ac.in

***Abstract*—Energy efficiency is a critical requirement in low-power wireless sensor networks. In this work, energy-efficient scheduling policies that exploit the temporal variation of wireless channel are presented. The proposed policies avoid regular feedback from the sensor nodes in order to decide on the channel access opportunity and the access duration. The policies cater to delay-tolerant as well as delay-constrained scenarios. The numerical results demonstrate that the proposed policies simultaneously offer a gain of about 20% in data throughput and about 58% in energy efficiency over the nearest competitive approaches. It is also shown that the performance of the scheduling policy corresponding to the delay-constrained scenario is bounded by the policy corresponding to the delay-unconstrained scenario.**

I. Introduction and Motivation

Ever-increasing growth of global Internet traffic in the past decade [1] has led to ubiquitous presence of low-power wireless devices, catering to a variety of applications. This increasing Internet traffic eventually leads to a proportionate increased energy consumption of these devices, which is unaffordable in energy-constrained application scenarios, such as in wireless sensor networks (WSNs) and Internet of Things (IoT). As a result, energy-efficient green communication [2], [3] has attracted a lot of attention in the recent years.

The core principle of green communication is to enhance the system energy efficiency without sacrificing data throughput. To meet this objective, an intelligent radio resource management module is required, of which the scheduler forms an integral part. The scheduler at the medium access control (MAC) layer essentially handles the dynamic allocation of radio resource to the sensor nodes (SNs). Once the resource allocation is done, the selected SN intelligently decides how carry out the communication process in the designated time.

Link scheduling in wireless networks is a well researched topic. The main challenge of scheduling [4], [5], [6] is the proper allocation of resources to all users of the network, such that it does not affect their desired Quality of Experience (QoE). Given that QoE is a measure from the users' perspective, it has a strong relation with the traditional underlying Quality of Service (QoS) in networks [7]. Thus, QoE requirements of an user refer to a scheme that jointly involves link scheduling as well as packet transmission. The authors in [4] demonstrated a thorough comparative analysis of different scheduling algorithms. The work in [5] analyzed the impact of various QoE requirements on various scheduling policies. It also proposed a novel scheduling policy for delay-constrained scenarios. The authors in [6] proposed a scheduling and link adaptation scheme for narrow-band IoT systems. It is notable that all these scheduling policies require regular channel state information (CSI) for decision-making, and also the channel assignment is done for single slot duration.

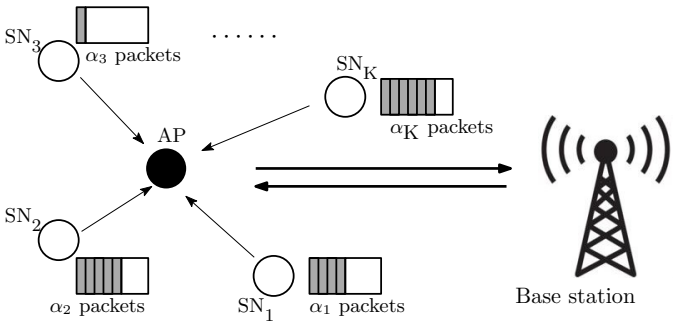

Fig. 1. System model illustrating a multi-access scenario.

Channel assignment is followed by the actual communication. There have been some research in the direction of channel-aware link-layer transmission schemes in this context. In [8], channel sensing at predetermined intervals was proposed, where communication takes place only if the channel state is found to be above a particular threshold. The study in [9] has considered channel dynamics aware feedback for point-to-point communication over wireless channel.

In this work, channel-aware scheduling policies are proposed for multi-access scenarios. The proposed policies avoid regular CSI feedback, thereby resulting in considerable performance enhancement in comparison with the other existing approaches in literature, with approximately 20% higher data throughput and 58% more energy efficiency.

II. System Model

A time-slotted synchronous system (slot duration T_p) is considered with K sensor nodes (SN), an access point (AP), and a base station (BS), as shown in Fig 1. AP communicates with BS over a dedicated channel. AP has only one channel under its command to gather information from the SNs, and hence it needs to intelligently decide which SN should be granted access to the channel and for how long.

Each SN k at any point of time has α_k packets of data to transmit with φ_k bits in each packet and the corresponding queueing delay constraint is D_k. Let Φ_K denote the set of

K SNs, i.e., $\Phi_K = \{\text{SN}_1, \text{SN}_2, \cdots, \text{SN}_K\}$. At any particular point of time, AP assigns the channel to one of the members of Φ_K. The problem revolves round the question as to how this channel assignment is to be done.

A. AP Activity

In order to decide which SN should be given access to the channel, AP requests CSI and queue information from the SNs that are associated to it. By queue information, it implies the values of α_k, φ_k, and D_k. Note that φ_k and D_k could be known a priori, based on the node's interest and its data type. In that case, the only variable of interest is α_k. Assuming the transmission power of all SNs to be identical, i.e., $P_{t,k} = P_t$ $\forall\ k = 1, \cdots, K$, received signal envelope at AP for SN_k is

$$X_k(t) = \sqrt{P_t}|h_k(t)| \quad \forall \quad k = 1, \cdots, K. \tag{1}$$

Here $h_k(t)$ is the circularly symmetric complex Gaussian (CSCG) channel gain between SN_k and AP. Accordingly, the complete set of information on SN_k is represented as the quintuple $\Psi_k = \{X_k(t), f_{d,k}, \alpha_k, \varphi_k, D_k\}$, where $f_{d,k}$ is the maximum Doppler frequency corresponding to SN_k. This quintuple is sent through a dedicated control channel.

$f_{d,k} \cong \frac{v_k f_c}{c}$, where v_k is node mobility, f_c is carrier frequency, and c is the signal velocity in vacuum. The quantity $f_{d,k}T_p$ characterizes the temporal variation of SN_k-AP channel; its large value indicates nearly-independent 'fast' fading channel, whereas $f_{d,k}T_p < 0.1$ implies a correlated 'slow' fading channel [10]. The received signal at AP can experience Doppler effect even with stationary AP and SN_k[11]; v_k, i.e., $f_{d,k}$ effectively captures the effect of mobility of Tx, Rx, or scatterers, or a combination of them. Thus, it also portrays wireless communication scenarios like IoT, where SNs may be static and scatterers are the prime causes of Doppler shift.

Based on Ψ_k, AP decides which SN should be assigned the channel and for how long.

B. SN Rate Adaptation

Each SN_k choose their appropriate constellation from a constellation set $\mathcal{C}_k = \{c_{k,1}, c_{k,2}, \cdots, c_{k,|\mathcal{C}|}\}$ with $c_{k,1} < c_{k,2} < \cdots < c_{k,|\mathcal{C}|} < \infty$, and $c_{k,1}$ signifying no transmission. The $|\mathcal{C}_k|$ transmission rates are accordingly $R_{k,j} = \log_2(c_{k,j})$ bits/symbol $\forall\ j = 1, \cdots, |\mathcal{C}|$, where $\log_2(c_{k,1}) = 0$.

The entire range of X_k (index t is removed for brevity) is divided into $|\mathcal{C}_k|$ regions with thresholds X_{T_k} $\forall\ k = 0, \cdots, |\mathcal{C}_k - 2|$ and each region being mapped to a constellation $c_{k,j}$. Bit error rate (BER) P_b, constellation $c_{k,j}(i)$, transmit power P_t, and SN_k−AP complex channel gain $h_k(i)$ in the i^{th} time slot are related as [12]:

$$P_b = a_1 \exp\left(\frac{-a_2 P_t |h_k(i)|^2}{N_0 B(j^{a_3}(i) - a_4)}\right), \tag{2}$$

where $a_1, \cdots, a_4$ are modulation-specific constants, N_0 is the noise spectral density, and B is the channel bandwidth.

If SN_k transmits with power P_t and uses constellation $c_{k,j}$, time slots needed for sending α_k packets with φ_k bits/packet is $\tau_{\text{req}}^{k,j} = \left\lceil \frac{\alpha_k \varphi_k}{R_{k,j}} \right\rceil$, where k and j respectively denote SN and constellation size index. Accordingly, the energy required is

$$E_{\text{req}}^{k,j} = (P_t + P_{\text{idle}})\tau_{\text{req}}^{k,j} T_p, \tag{3}$$

where P_{idle} is the power required for circuit operation. Note that $E_{\text{req}}(j)$ is a function of $c_{k,j}$, which jointly depends on the selected SN and the modulation used.

C. Duration of Stay (DoS) Estimation

Let $X_k(t) = X_{k,0}$ and $X_{k,0} \in [X_{T_i}, X_{T_{i+1}})$ without any loss of generality. Based on $f_{d,k}$ and T_p, AP estimates the time $\zeta_{k,i}$ (in slots) for which X_k will continue to stay in $[X_{T_i}, X_{T_{i+1}})$ with a probability $1 - \epsilon_0$, where ϵ_0 is the acceptable error limit [9] and index i indicates the usage of i^{th} modulation scheme. Details of DoS $\zeta_{k,i}$ estimation are presented in Appendix A.

DoS estimation will play a crucial role in the proposed policies in this paper, as discussed next.

III. Proposed Framework

A scheduling framework is now proposed, for delay-constrained (i.e., D_k is finite $\forall\ k = 1, \cdots, K$) as well as delay-unconstrained data (i.e., $D_k \to \infty\ \forall\ k = 1, \cdots, K$).

A. Delay constrained scenario (DCS)

Here, a new framework is proposed for deciding the channel allocation among Φ_K, where SN_k $\forall\ k = 1, \cdots, K$ is handling delay constrained data. The framework aims at enhancing the system energy efficiency as follows:

1) AP requests the K SNs to send their respective quintuple $\Psi_k = \{X_k(t), f_{d,k}, \alpha_k, \varphi_k, D_k\}$ $\forall\ k = 1, \cdots, K$.
2) The channel is assigned to a particular SN of Φ_K based on the following criteria: Optimal SN (SN_{opt}) is chosen from Φ_K according to the optimization problem P1:

$$\text{(P1)} \quad : \underset{k,i}{\text{minimize}}\ D_k - \min\left(\tau_{\text{req}}^{k,i}, \zeta_{k,i}\right) \tag{4}$$

$$\text{subject to} \quad C1 : k \in \{1, \cdots, K\}, \quad \text{and}$$

$$C2 : i \in \{1, \cdots, |\mathcal{C}|\}.$$

SN_{opt} is that particular SN from Φ_K, which minimizes the objective function of P1 according to $C1$ and $C2$. Note that this assignment is for the time interval

$$T_{\text{opt}} = \min\left(\tau_{\text{req}}^{k_{\text{opt}}, i_{\text{opt}}}, \zeta_{k_{\text{opt}}, i_{\text{opt}}}\right), \tag{5}$$

during which SN_{opt} transmits data using modulation level i_{opt} to AP.
3) AP notifies SN_{opt} about its selection and also that it has been granted channel access for the next T_{opt} duration.
4) $\Phi_K \backslash \{\text{SN}_{\text{opt}}\}$ are notified about T_{opt}, based on which they update their delay constraint D_k as $D_k' = D_k - T_{\text{opt}}$ and enter 'sleep mode' for this entire duration. Note that this monotonically decreasing nature of D_k $\forall\ k = 1, \cdots, K$ guarantees timely delivery of data packets of all the SNs.
5) AP again sends the Ψ request to all SNs after time T_{opt} for determining the next cycle of this process and the SNs with data to transmit participate.

Remark 1: When multiple SNs have identical remaining time, i.e., $D_k - \min\left(\tau_{\text{req}}^{k,i}, \zeta_{k,i}\right) = T_{\text{opt}}$ for multiple k, the SN corresponding to the lowest $\min\left(\tau_{\text{req}}^{k,i}, \zeta_{k,i}\right)$ is assigned the channel for the next T_{opt} duration.

Remark 1 guarantees that in case of a deadlock, SN having the best channel condition is always given an upper-hand.

Remark 2: Unlike the existing scheduling frameworks, the proposed framework is jointly queue and channel aware in nature. While $D_k \ \forall \ k = 1, \cdots, K$ guarantees time-bound data delivery, $\zeta_{k,i}$ takes care of the 'channel' factor.

B. Delay unconstrained scenario (DUCS)

As dealing with delay-tolerant data is considered here, $D_k \to \infty \ \forall \ k = 1, \cdots, K$. Hence, the quintuple Ψ_k reduces to $\Psi_k = \{X_k(t), f_{d,k}, \alpha_k, \varphi_k\} \ \forall \ k = 1, \cdots, K$. The proposed framework is as follows:

1) As in the previous section, here also AP requests all the SNs to send their respective $\Psi_k \ \forall \ k = 1, \cdots, K$.
2) The optimal SN, i.e., SN_{opt} is that particular SN from Φ_K, which maximizes the objective of the following optimization problem P2:

$$\text{(P2)} \quad : \underset{k,i}{\text{maximize}} \ \zeta_{k,i} R_{k,i}[1 - P_b](1 - \epsilon_0) \tag{6}$$

subject to $C1$ and $C2$.

SN_{opt} is assigned the channel for the entire duration of T_{opt} from (5), during which it transmits data using modulation level i_{opt} to AP.

3) AP notifies SN_{opt} about its selection and also that it has been granted access for the next T_{opt} duration.
4) $\Phi_K \backslash \{\text{SN}_{\text{opt}}\}$ are notified about T_{opt}, based on which they enter 'sleep mode' for this entire duration.
5) AP again sends the Ψ request to all SNs after duration T_{opt} for determining the next cycle of this process and the SNs with data to transmit participate.

Remark 3: Unlike the existing scheduling mechanisms, the proposed mechanism is not periodic in nature. It depends on the estimated T_{opt}, which in turn depends on $\Psi_k \ \forall \ k = 1, \cdots, K$.

Remark 4: The proposed mechanism does not necessarily chose the SN with the best channel condition, but it chooses that SN, which maximizes the data transferred in T_{opt} duration.

SN_m, whose channel condition is $R_{m,i}$ transmission rate suitable for $\zeta_{m,i}$ slots is chosen over SN_n having $R_{n,j}$ transmission rate suitable channel for $\zeta_{n,j}$ slots even if $R_{m,i} < R_{n,j}$, provided $R_{m,i}\zeta_{m,i} > R_{n,j}\zeta_{n,j}$. In other words,

$$\frac{R_{k_{\text{opt}},i_{\text{opt}}}\zeta_{k_{\text{opt}},i_{\text{opt}}}}{R_{k,i}\zeta_{k,i}} > 1 \implies R_{k_{\text{opt}},i_{\text{opt}}} > R_{k,i} \quad \forall \ k \in K \backslash \{k_{\text{opt}}\}, \ i \in \{2, \cdots, |\mathcal{C}|\}. \tag{7}$$

Illustration: Suppose there are 2 SNs requesting AP for access, such that: SN_1 is 8-QAM suitable for 20 slots and SN_2 is 64-QAM suitable for 5 slots. In such a case, the proposed protocol grants access to SN_1 and not SN_2, because $\log_2(8) \cdot 20 > \log_2(64) \cdot 5$.

Theorem 1: For Φ_K with $K = 1$, SN_1 transmits $\alpha_1\varphi_1$ bits of data to AP in finite time $\mathbb{T}$, where

$$\mathbb{T} = \sum_{m=1}^{M} \zeta_{1,0}(m) + \sum_{\substack{n=1 \\ i \neq 0}}^{N-1} \zeta_{1,i}(n) + \frac{\alpha_1\varphi_1 - (1 - \epsilon_0)[1 - P_b] \sum\limits_{\substack{n=1 \\ i \neq 0}}^{N-1} \zeta_{1,i}(n) R_{1,i}(n)}{R_{1,i_N}[1 - P_b]}, \tag{8}$$

where $M, N \in \mathbb{N}$.

Proof 1: Please see Appendix B.

Theorem 1 guarantees that if the data is delay-tolerant in nature, it will always be delivered to AP in finite time irrespective of the variations in wireless channel.

IV. Performance Measures

Without any loss of generality, assume data frames are of constant size, single slot long, i.e., $T_f = T_p$. Probing packets are assumed to be very small, i.e., $T_{pr} = \delta T_p \ (\delta \ll 1)$ [13].

AP at any point of time assigns the channel to SN_k for time duration $\theta_{k,i}$, during which SN_k employs modulation index i. Accordingly, define 'system energy efficiency' η as $\eta = \frac{\mathcal{D}_{\mathcal{R}}}{\mathcal{E}_{\mathcal{C}}}$, where $\mathcal{D}_{\mathcal{R}}$ is the system data throughput and $\mathcal{E}_{\mathcal{C}}$ is the energy consumption. Under this model, the system data-throughput and energy efficiency are expressed as:

A. Data throughput $\mathcal{D}_{\mathcal{R}}$

$\mathcal{D}_{\mathcal{R}}$ is defined as the long-term average of successful data transmissions per unit time per sensor node, i.e.,

$$\mathcal{D}_{\mathcal{R}} = \lim_{N \to \infty} \frac{(1 - \epsilon_0) \sum\limits_{n=1}^{N} \sum\limits_{k=1}^{K} \zeta_{k,i}(n) R_{k,i}(n)[1 - P_b(n)] \Omega_{k,n}}{\sum\limits_{n=1}^{N} \sum\limits_{k=1}^{K} (\theta_{k,i} + 3T_{pr}) \Omega_{k,n}}. \tag{9}$$

Here $R_{k,i}(n)[1 - P_b(n)]$ is the data throughput associated with modulation level i when the acceptable BER is $P_b(n)$ [14], $\theta_{k,i} = \zeta_{k,i}T_p$, $3T_{pr}$ accounts for the AP-SN handshake, and $\Omega_{k,n} \in \{0, 1\}$ is an indicator variable which guarantees that only one SN can be chosen at any particular point of time, i.e., $\sum\limits_{k=1}^{K} \Omega_{k,n} = 1 \ \forall \ n = 1, \cdots, N$. Note that though the acceptable BER varies depending on the application at hand, it remains constant throughout any particular application. In other words, $P_b(n) = P_b \ \forall \ n = 1, \cdots, N$.

B. Energy consumption $\mathcal{E}_{\mathcal{C}}$

$\mathcal{E}_{\mathcal{C}}$ is defined as the long term energy consumption per unit time per sensor node, i.e.,

$$\mathcal{E}_{\mathcal{C}} = \lim_{N \to \infty} \frac{\sum\limits_{n=1}^{N} \sum\limits_{k=1}^{K} e_{n,k}}{\sum\limits_{n=1}^{N} \sum\limits_{k=1}^{K} \theta_{k,i} \Omega_{k,n}}, \tag{10}$$

TABLE I
THRESHOLDS (DBM) FOR VARIOUS BER

Modulation \ BER	10^{-9}	10^{-7}	10^{-5}	10^{-3}	10^{-1}
No transmission	$X_{k,0} < 11.54$	$X_{k,0} < 10.50$	$X_{k,0} < 9.11$	$X_{k,0} < 6.98$	$X_{k,0} < 3.00$
BPSK	$X_{k,0} \in [11.54, 14.56)$	$X_{k,0} \in [10.50, 13.51)$	$X_{k,0} \in [9.11, 12.12)$	$X_{k,0} \in [6.98, 10.00)$	$X_{k,0} \in [3.00, 6.01)$
QPSK	$X_{k,0} \in [14.56, 16.32)$	$X_{k,0} \in [13.51, 15.27)$	$X_{k,0} \in [12.12, 13.88)$	$X_{k,0} \in [10.00, 11.76)$	$X_{k,0} \in [6.01, 7.78)$
8-QAM	$X_{k,0} \in [16.32, 17.57)$	$X_{k,0} \in [15.27, 16.52)$	$X_{k,0} \in [13.88, 15.13)$	$X_{k,0} \in [11.76, 13.01)$	$X_{k,0} \in [7.78, 9.02)$
16-QAM	$X_{k,0} \in [17.57, 18.54)$	$X_{k,0} \in [16.52, 17.48)$	$X_{k,0} \in [15.13, 16.10)$	$X_{k,0} \in [13.01, 13.97)$	$X_{k,0} \in [9.02, 9.99)$
32-QAM	$X_{k,0} \in [18.54, 19.33)$	$X_{k,0} \in [17.48, 18.28)$	$X_{k,0} \in [16.10, 16.89)$	$X_{k,0} \in [13.97, 14.77)$	$X_{k,0} \in [9.99, 10.79)$
64-QAM	$19.33 \leq X_{k,0}$	$18.28 \leq X_{k,0}$	$16.89 \leq X_{k,0}$	$14.77 \leq X_{k,0}$	$10.79 \leq X_{k,0}$

where $e_{n,k} = K(3\mathcal{P}_p + 2\mathcal{P}_r)T_{pr} + \mathcal{P}_p T_{pr} + \theta_{k,i}(n)\Omega_{k,n}[\mathcal{P}_t + (K-1)\mathcal{P}_s]$. $\mathcal{P}_p$ denotes the probing signal power consumption, $\mathcal{P}_t$ (respectively, $\mathcal{P}_r$) is the transmit (respectively, receive) power, and $\mathcal{P}_s$ being the power-saving mode consumption.

With the mathematical definitions of $\mathcal{D}_\mathcal{R}$ and $\mathcal{E}_\mathcal{C}$ in (9) and (10), energy efficiency $\eta = \dfrac{\mathcal{D}_\mathcal{R}}{\mathcal{E}_\mathcal{C}}$ can be computed.

V. NUMERICAL RESULTS

In this section, performance of the proposed framework is illustrated. Though the results presented here consider Rayleigh fading scenario, the claims are valid for all underlying fading distributions. Default system parameters: carrier frequency $f_c = 900$ MHz, $T_p = 100$ μs, and $\delta = 0.1$.

A 5 SN multi-access scenario is considered, with node velocity $10, 14, 16, 18,$ and 20 kmph, respectively. Note that the main application of the proposed scheduling policies is scenarios like IoT, where SNs are statically placed and the Doppler effect is mainly due to the scatterers. This is the reason behind choosing moderate and not high node velocity values. Moreover, this is also a practical scenario, as considering unequal node velocity will result in unequal $f_{d,k}$ $\forall$ $k = 1, \cdots, 5$. The delay limit is considered as $D_k = 50$ ms $\forall$ $k = 1, \cdots, 5$ [15]. Considering short range communication, the propagation delay is ignored. Energy consumption parameters are taken from Microchip ATZB-900-B0R datasheet [16]: $\mathcal{P}_t, \mathcal{P}_p = 60$ mW, $\mathcal{P}_r = 45$ mW, and $\mathcal{P}_s = 18$ mW. From (2), $P_b = 2\exp\left(\dfrac{-1.5P_t|h_k(i)|^2}{N_0 B(j(i)-1)}\right)$ for M-QAM constellations [12]. Without any loss of generality, $N_0 B = 1$ is considered.

A. Effect of System Parameters

Fig. 2 depicts the variation of energy efficiency η of the proposed scheduling policies, namely DCS and DUCS, with BER P_b. It is observed that, though η initially increases with increasing P_b, it reaches an optimum value at around $P_b = 10^{-3}$ before it starts decreasing. The reason is as follows:

It is observed from Table I that a higher modulation index is assigned to the same $X_{k,0}$ for $P_b = p_1$ against $P_b = p_2$, when $p_1 > p_2$. For example, $X_{k,0} = 10.8$ dBm is assigned no transmission when $P_b = 10^{-9}$ compared to $P_b = 10^{-1}$, when 64-QAM is assigned for the same $X_{k,0}$. This results in initial increase in η against P_b. However, recall that data rate corresponding to a modulation level j is $R_j(1 - P_b)$. When $P_b \ll 1$, it does not affect the data rate and it is approximately R_j. On the contrary, $(1-P_b)$ contributes significantly when P_b is high, i.e., the effect of P_b dominates as its value increases, and this is the reason for which η decreases after a certain P_b.

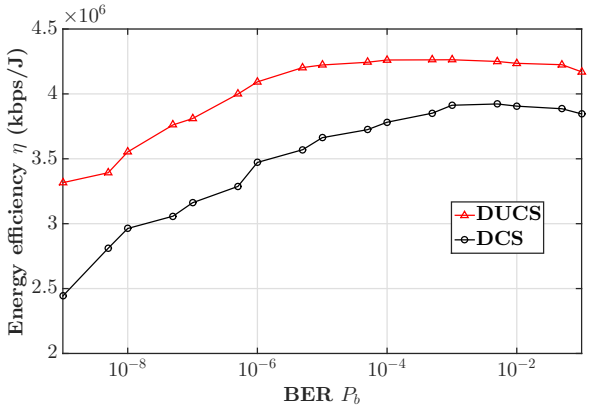

Fig. 2. Variation of energy efficiency with BER. $\epsilon_0 = 0.05$.

It may also be noted that DUCS outperforms DCS in terms of energy efficiency. The reason behind such an occurrence is the fact that DUCS maximizes the 'individual performance', while DCS guarantees that the QoS constraint (in this case, delay D_k $\forall$ $k = 1, \cdots, K$) is not violated.

Illustration: Suppose SN_m and SN_n are contending for the channel among K SNs, with their respective DoS being $\zeta_{m,p}$ and $\zeta_{n,q}$ respectively. With $\tau_{\text{req}}^{m,p} > \zeta_{m,p}$ and $\tau_{\text{req}}^{n,q} > \zeta_{n,q}$, the objective of P1 changes to $D_k - \zeta_{k,i}$ $\forall$ $k \in \{m, n\}$, $i \in \{1, \cdots, |\mathcal{C}|\}$. As P1 aims at minimization of the objective function, it is obvious that $\max\{\zeta_{m,p}, \zeta_{n,q}\}$ will be selected. But as demonstrated by the illustration following Remark 4, it can be noted that having $\zeta_{m,p} > \zeta_{n,q}$ does not guarantee $R_{m,p}\zeta_{m,p} > R_{n,q}\zeta_{n,q}$. In other words,

while P1 guarantees time-bound data transfer, it does not guarantee maximum utilization of the channel, i.e., DCS will choose SN_m over SN_n if $\zeta_{m,p} > \zeta_{n,q}$ even if $R_{m,p}\zeta_{m,p} < R_{n,q}\zeta_{n,q}$. This results in lower $\mathcal{D}_\mathcal{R}$ and η compared to its delay unconstrained counterpart DUCS.

To quantify the trade-off between enhanced energy efficiency and timeliness of data transfer, the channel occupancy of the 5 SNs is empirically characterized. Two cases of $P_b = 10^{-8}$ and $P_b = 10^{-6}$ are considered and the variance of channel occupancy among the 5 SNs are obtained.

Table II demonstrates the channel occupancy variance for both DCS and DUCS in two different P_b scenarios. It is notable

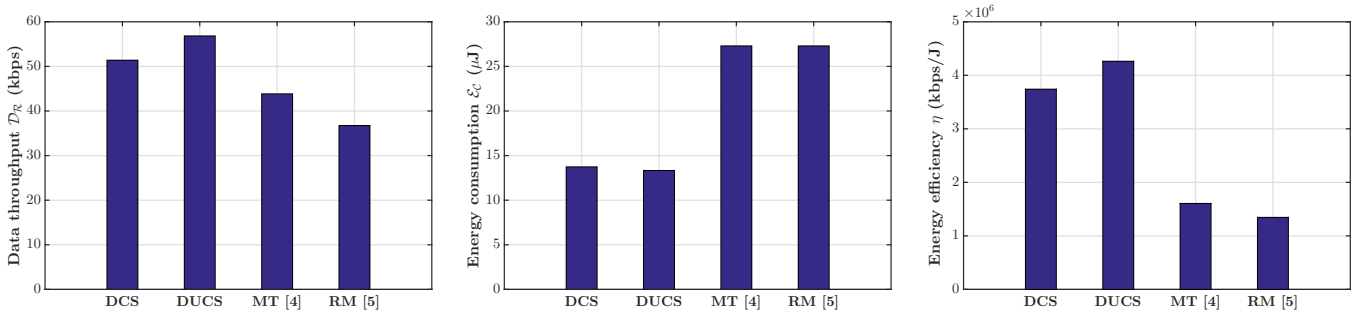

(a) (b) (c)

Fig. 3. Performance comparison: (a) Data throughput; (b) Energy consumption; (c) Energy efficiency. $\epsilon_0 = 0.05$.

TABLE II
VARIATION OF CHANNEL OCCUPANCY

Scheme \ BER	10^{-8}	10^{-6}
DCS	1.3456	0.8156
DUCS	11.4124	3.7232

that the variance in case of DUCS is approximately 9 and 4 times compared to DCS for $P_b = 10^{-8}$ and 10^{-6} respectively. In other words, channel occupancy among the various SNs is significantly skewed in DUCS compared to DCS, i.e., all SNs do not get equal access to the channel in DUCS unlike DCS.

For a given application, P_b is fixed at a particular value. This has motivated to consider a fixed value of P_b $(= 10^{-4})$ for the study in next section, where DCS and DUCS performances are compared with respect to the existing approaches.

B. Performance Comparison

First, the various other competitive approaches, namely MTS and RTBM are briefly discussed:

1) Maximum Throughput Scheduler (MT) [4]: This is the opportunistic scheduler, i.e., exploits CSI to schedule the SN with most favorable channel condition.
2) Remaining Time Based Maximal Scheduler (RM) [5]: It performs scheduling based on the 'remaining time' constraint for each SN, i.e, the maximum delay a task at a SN can suffer without violating the QoS requirement.

Please note, both MT and RM regularly require CSI at the AP to decide on the scheduling process.

1) Data throughput $\mathcal{D}_\mathcal{R}$: Fig. 3(a) exhibits that the proposed scheduling policies, DCS and DUCS perform significantly better than MT and RM. In particular, DCS and DUCS offer 17.19% and 29.63% higher data throughput respectively compared to their nearest competitor MT. This enhancement in performance can be attributed to the way in which the CSI knowledge is used in both DCS and DUCS, because both MT and RM also require CSI, but still they are not able to perform as efficiently as the proposed scheduling policies.

2) Energy consumption $\mathcal{E}_\mathcal{C}$: Fig. 3(b) demonstrates that $\mathcal{E}_\mathcal{C}$ corresponding to both DCS and DUCS is significantly lesser ($\sim 42\%$) compared to both MT and RM. The reason behind such an observation is that, both DCS and DUCS intelligently exploits the knowledge of the dynamically varying wireless channel unlike MT and RM, and hence, avoids regular CSI feedback at the AP. This results in significant energy saving, which is extremely crucial in energy-constrained scenarios.

3) Energy efficiency η: Fig. 3(c) shows that both MT and RM offer η in the range of $\sim 1.4 \times 10^9$ kbps/J, which is approximately 58% lesser compared to both DCS and DUCS. When this fact is combined along with approximately 20% higher data throughput and approximately 42% lower energy consumption, enhanced performance of the proposed scheduling policies is demonstrated.

Lastly, as also observed in Section V-A, DUCS outperforms DCS on all performance metrics, namely, $\mathcal{D}_\mathcal{R}, \mathcal{E}_\mathcal{C}$, and η.

VI. CONCLUSION

In this work, channel-aware dynamic feedback-based scheduling policies, called DCS and DUCS, have been proposed for multiple access channels. The proposed policies exploit the channel knowledge information and avoid regular CSI feedback at the AP. As DUCS deals with delay-tolerant data delivery, unlike DCS it results in enhanced performance in terms of both higher data rate and energy efficiency, and lower energy consumption. However, DUCS does not guarantee timely data delivery like DCS. DCS achieves the delay guarantee at the cost of a little degraded performance, i.e., DCS focuses on maximizing the 'social good' while DUCS focuses on the 'individual good'. It has been observed that both DCS and DUCS significantly outperform the existing competitive approaches, namely MT and RM. Overall, both DCS and DUCS offer an average data throughput improvement of 20% and energy efficiency enhancement of approximately 58% compared to the competitive approaches. Lastly, note that the proposed scheme is centralized in nature, and hence computational complexity increases with increase in the number of SNs. As an extension, we intend to explore this aspect in future and propose its computationally efficient distributed counterpart.

APPENDIX A
$\zeta_{k,i}$ ESTIMATION

The time derivative of X_k, i.e., $\dot{X}_k \triangleq \frac{dX_k(t)}{dt}$ is a zero mean Gaussian random variable (RV) irrespective of the underlying fading distribution, i.e., $\dot{X}_k \sim \mathcal{N}(0, \dot{\sigma})$ [17], where $\dot{\sigma}$ is dependent on the probability distribution function of X_k. Accordingly, if $X_{k,1}$ $(= \dot{X} \cdot T_p)$ is defined as the temporal variation of X_k in the immediate slot, $X_{k,1}$ follows a truncated Gaussian distribution in $[-X_{k,0}, \infty)$ [18]:

$$f_{X_{k,1}}(\beta) = \begin{cases} \frac{1}{1-\Phi_1\left(-\frac{X_0}{\dot{\sigma}_1}\right)} \frac{1}{\sqrt{2\pi}\dot{\sigma}_1} e^{\left(\frac{-\beta^2}{2\dot{\sigma}_1{}^2}\right)} & -X_{k,0} \leq \beta \\ 0 & \text{elsewhere.} \end{cases} \quad (11)$$

Here $\Phi_1(x) = \int_{-\infty}^{x} \frac{1}{\sqrt{2\pi}} e^{-\frac{t^2}{2}} dt$ is the cumulative distribution function of standard univariate normal distribution.

DoS $\zeta_{k,i}$ is obtained by solving the optimization problem P3 [9, Equation 10]:

$$\text{(P3)} \quad : \underset{\zeta_{k,i} \geq 0}{\text{maximize}} \ \zeta_{k,i} \qquad \text{subject to} \quad \epsilon(\zeta_{k,i}) \leq \epsilon_0, \quad (12)$$

where

$$\epsilon(\zeta_{k,i}) = 1 - \Pr\left\{X_{T_i} \leq X_{k,0} + X_{k,1} < X_{T_{i+1}}, \cdots, X_{T_i} \leq X_{k,0} + X_{k,\zeta_{k,i}} < X_{T_{i+1}}\right\}.$$

Here $X_{k,p}$ $\forall$ $p = 2, \cdots, \zeta$ are truncated zero mean Gaussian R.Vs in $[-X_{k,0}, \infty)$ with $\dot{\sigma}_i^2 = i \cdot \dot{\sigma}_1$.

Proposition 1: $X_m = X_{m,0} \in [X_{T_i}, X_{T_{i+1}})$, $X_n = X_{n,0} \in [X_{T_i}, X_{T_{i+1}})$ $\forall$ $m, n = 1, \cdots, K$ does not necessarily imply $\zeta_{m,i} = \zeta_{n,i}$, even for identical set of system parameters. It only guarantees that the modulation level i is to be used.

Proof 2: It is observed from (11) that, to solve (12) one needs to evaluate integrals over truncated Gaussian RVs. Even if $X_{m,0}, X_{n,0} \in [X_{T_i}, X_{T_{i+1}})$, it does not necessarily translate to having identical regions of integration. In other words,

$$X_{m,0}, X_{n,0} \in [X_{T_i}, X_{T_{i+1}}) \implies [-X_{m,0}, \infty) \equiv [-X_{n,0}, \infty). \quad (13)$$

This dissimilarity results in having $\zeta_{m,i} \neq \zeta_{n,i}$, even if $X_{m,0}, X_{n,0} \in [X_{T_i}, X_{T_{i+1}})$ $\forall$ $m, n = 1, \cdots, K$.

APPENDIX B
PROOF OF THEOREM 1

We prove the theorem in three sub-parts.

A. From Appendix A it is known that even if $X_{k,0} \in [X_{T_0}, X_{T_1})$, X_k is bound to leave $[X_{T_0}, X_{T_1})$ in finite time, i.e., $\zeta_{k,0}$ is always a finite value. It not only guarantees a finite $\zeta_{1,0}$, but it also guarantees a finite number of such instances. Accordingly, the first term $\sum_{m=1}^{M} \zeta_{1,0}(m)$, which represents the total time during which SN_1 avoids channel usage in the process of transferring $\alpha_1\varphi_1$ bits to AP is a finite quantity.

B. $\zeta_{1,i}$ $\forall$ $i \neq 0$ indicates the estimated duration for which SN_1 uses modulation level i $(i \neq 0)$ when $X_{1,0} \in [X_{T_i}, X_{T_{i+1}})$. Thus, the second term represents the time duration that SN_1 uses to successfully communicate $(1-\epsilon_0)[1 - P_b] \sum_{\substack{n=1 \\ i \neq 0}}^{N-1} \zeta_{1,i}(n) R_{1,i}(n)$ bits of data to AP. Note that N is practically a finite quantity, as $\alpha_1\varphi_1$ is always a finite quantity.

C. The last term is essentially the single partial transmission slot, as transmission may stop anywhere within $\zeta_{1,i}(N)$ depending on $\alpha_1\varphi_1$ and data successfully communicated over previous $N-1$ $\zeta_{1,i}$, where $i \neq 0$. This completes the proof.

REFERENCES

[1] "On the pulse of the networked society," Ericsson Mobility Report, Nov. 2018.

[2] J. Xu, L. Duan, and R. Zhang, "Cost-aware green cellular networks with energy and communication cooperation," *IEEE Commun. Mag.*, vol. 53, no. 5, pp. 257–263, May 2015.

[3] Q. Wu, G. Y. Li, W. Chen, D. W. K. Ng, and R. Schober, "An overview of sustainable green 5G networks," *IEEE Wireless Commun.*, vol. 24, no. 4, pp. 72–80, Aug. 2017.

[4] O. Grøndalen, A. Zanella, K. Mahmood, M. Carpin, J. Rasool, and O. N. Østerbø, "Scheduling policies in time and frequency domains for LTE downlink channel: A performance comparison," *IEEE Trans. Veh. Technol.*, vol. 66, no. 4, pp. 3345–3360, Apr. 2017.

[5] X. Zheng, Z. Cai, J. Li, and H. Gao, "A study on application-aware scheduling in wireless networks," *IEEE Trans. Mobile Comput.*, vol. 16, no. 7, pp. 1787–1801, July 2017.

[6] C. Yu, L. Yu, Y. Wu, Y. He, and Q. Lu, "Uplink scheduling and link adaptation for narrowband internet of things systems," *IEEE Access*, vol. 5, pp. 1724–1734, 2017.

[7] M. Fiedler, T. Hossfeld, and P. Tran-Gia, "A generic quantitative relationship between quality of experience and quality of service," *IEEE Netw.*, vol. 24, no. 2, pp. 36–41, Mar. 2010.

[8] H. Moon, "Channel-adaptive random access with discontinuous channel measurements," *IEEE J. Sel. Areas Commun.*, vol. 34, no. 5, pp. 1704–1712, May 2016.

[9] P. Mukherjee and S. De, "Dynamic feedback based adaptive modulation for energy-efficient communication," *IEEE Commun. Lett.*, vol. 23, no. 5, pp. 946–949, May 2019.

[10] M. Zorzi, R. R. Rao, and L. B. Milstein, "ARQ error control for fading mobile radio channels," *IEEE Trans. Veh. Technol.*, vol. 46, no. 2, pp. 445–455, May 1997.

[11] A. Borhani and M. Pätzold, "Correlation and spectral properties of vehicle-to-vehicle channels in the presence of moving scatterers," *IEEE Trans. Veh. Technol.*, vol. 62, no. 9, pp. 4228–4239, Nov. 2013.

[12] A. Goldsmith, *Wireless Communications*. Cambridge University Press, 2005.

[13] M. Zorzi and R. R. Rao, "Error control and energy consumption in communications for nomadic computing," *IEEE Trans. Comput.*, vol. 46, no. 3, pp. 279–289, Mar. 1997.

[14] Q. Liu, S. Zhou, and G. B. Giannakis, "Queuing with adaptive modulation and coding over wireless links: cross-layer analysis and design," *IEEE Trans. Wireless Commun.*, vol. 4, no. 3, pp. 1142–1153, May 2005.

[15] K. A.M, F. Hu, and S. Kumar, "Intelligent spectrum management based on transfer actor-critic learning for rateless transmissions in cognitive radio networks," *IEEE Trans. Mobile Comput.*, vol. 17, no. 5, pp. 1204–1215, May 2018.

[16] ATZB-900-B0R Datasheet, Microchip. [Online]. Available: http://ww1.microchip.com/downloads/en/DeviceDoc/doc8227.pdf (Access date: Apr. 2019).

[17] S. L. Cotton, "Second-order statistics of $\kappa - \mu$ shadowed fading channels," *IEEE Trans. Veh. Technol.*, vol. 65, no. 10, pp. 8715–8720, Oct. 2016.

[18] P. Mukherjee, D. Mishra, and S. De, "Gaussian mixture based context-aware short-term characterization of wireless channels," *IEEE Trans. Veh. Technol.*, vol. 69, no. 1, pp. 26–40, Jan. 2020.